Acta Biomaterialia 10 (2014) 5055–5063

Contents lists available at ScienceDirect

Acta Biomaterialia

journal homepage: www.elsevier.com/locate/actabiomat

Material properties of components in human carotid atherosclerotic plaques: A uniaxial extension study

Zhongzhao Teng [a,b,*], Yongxue Zhang [c,a], Yuan Huang [a], Jiaxuan Feng [c], Jianmin Yuan [a], Qingsheng Lu [c], Michael P.F. Sutcliffe [b], Adam J. Brown [d], Zaiping Jing [c], Jonathan H. Gillard [a]

[a] Department of Radiology, University of Cambridge, School of Clinical Medicine, Box 218 Cambridge Biomedical Campus, Cambridge CB2 0QQ, UK
[b] Department of Engineering, University of Cambridge, UK
[c] Department of Vascular Surgery, Changhai Hospital, Shanghai, People's Republic of China
[d] Division of Cardiovascular Medicine, University of Cambridge, UK

ARTICLE INFO

Article history:
Received 29 April 2014
Received in revised form 31 July 2014
Accepted 1 September 2014
Available online 6 September 2014

Keywords:
Atherosclerosis
Material property
Lipid
Haemorrhage
Thrombus

ABSTRACT

Computational modelling to calculate the mechanical loading within atherosclerotic plaques has been shown to be complementary to defining anatomical plaque features in determining plaque vulnerability. However, its application has been partially impeded by the lack of comprehensive knowledge about the mechanical properties of various tissues within the plaque. Twenty-one human carotid plaques were collected from endarterectomy. The plaque was cut into rings, and different type of atherosclerotic tissues, including media, fibrous cap (FC), lipid and intraplaque haemorrhage/thrombus (IPH/T) was dissected for uniaxial extension testing. In total, 65 media strips from 17 samples, 59 FC strips from 14 samples, 38 lipid strips from 11 samples, and 21 IPH/T strips from 11 samples were tested successfully. A modified Mooney–Rivlin strain energy density function was used to characterize the stretch–stress relationship. The stiffnesses of media and FC are comparable, as are lipid and IPH/T. However, both media and FC are stiffer than either lipid or IPH/T. The median values of incremental Young's modulus of media, FC, lipid and IPH/T at $\lambda = 1$ are 290.1, 244.5, 104.4, 52.9, respectively; they increase to 1019.5, 817.4, 220.7 and 176.9 at $\lambda = 1.1$; and 4302.7, 3335.0, 533.4 and 268.8 at $\lambda = 1.15$ (unit, kPa; λ, stretch ratio). The material constants of each tissue type are suggested to be: media, $c_1 = 0.138$ kPa, $D_1 = 3.833$ kPa and $D_2 = 18.803$; FC, $c_1 = 0.186$ kPa, $D_1 = 5.769$ kPa and $D_2 = 18.219$; lipid, $c_1 = 0.046$ kPa, $D_1 = 4.885$ kPa and $D_2 = 5.426$; and IPH/T, $c_1 = 0.212$ kPa, $D_1 = 4.260$ kPa and $D_2 = 5.312$. It is concluded that all soft atherosclerotic tissues are non-linear, and both media and FC are stiffer than either lipid or IPH/T.

1. Introduction

Stroke is the third leading cause of death globally [1], with carotid atherosclerotic disease responsible for 25–30% of cerebrovascular ischemic events in western nations [2]. Currently, carotid luminal stenosis is the only validated diagnostic criterion for risk stratification, but this criterion becomes less reliable in patients with mild to moderate stenoses. Clinical trials have shown that carotid endarterectomy (CEA) provides maximum benefit for patients with significant carotid stenoses ($\geqslant$70%), but the overall benefit of CEA becomes negligible when stenosis severity is reduced (<70%). Importantly, the majority of clinical events occur in patients with mild to moderate carotid stenoses [3,4]. Novel non-invasive diagnostic screening methods are urgently needed to identify vulnerable plaques earlier in an attempt to avoid acute ischemic events.

Atherosclerotic plaques are multicomponent structures composed of some, or all, of the following components: lipid, calcium, plaque haemorrhage (PH) and fibrous cap (FC). A typical vulnerable carotid plaque underlying a clinical event is frequently characterized by the presence of PH and FC rupture. These features can be quantified by in vivo medical imaging modalities, including high-resolution, multi-contrast magnetic resonance imaging (MRI) [5–7], and used to predict events in symptomatic [8,9] and asymptomatic [10,11] patients. In a meta-analysis of 31 histological studies, the prevalence of PH was increased in symptomatic vs. asymptomatic patients [12]. Similarly, in a recent meta-analysis of eight clinical studies of 689 patients, the hazard ratio of MRI-depicted PH in symptomatic patients was 11.7 [13]. FC rupture is

* Corresponding author at: Department of Radiology, University of Cambridge, School of Clinical Medicine, Box 218 Cambridge Biomedical Campus, Cambridge CB2 0QQ, UK. Tel.: +44 (0)1223 746447; fax: +44 (0)1223 330915.
E-mail address: zt215@cam.ac.uk (Z. Teng).

http://dx.doi.org/10.1016/j.actbio.2014.09.001
1742-7061/

also a common feature in symptomatic patients with a prevalence of ~60% [14]. In vivo imaging-based studies have demonstrated an association between FC rupture and subsequent events in symptomatic patients [8]. Event rates are increased when combinations of these two features are present [15]. Although 60–70% symptomatic patients exhibit PH or FC rupture at baseline [12,14,16], only ~15% will experience a recurrent event at one year [17,18]. From these results, it is clear that image-detected PH or FC rupture alone, or in combination, cannot serve as a robust marker for prospective cerebrovascular risk, and additional analyses or biomarkers are required.

Carotid atherosclerotic plaques continually undergo large deformations as a result of blood pressure and flow. From a material viewpoint, rupture could possibly occur when the external loading exceeds the plaques' material strength. Therefore, biomechanical analysis may provide complementary information to plaque structure and luminal stenosis in determining vulnerability. Previous results have shown that most rupture sites are also sites of increased mechanical stress [19–22]. Calculating mechanical stress within FC may help differentiate symptomatic and asymptomatic individuals [23–25] and could provide incremental information to predict subsequent ischemic cerebrovascular events in symptomatic patients in the carotid [26] and coronary [27]. These findings suggest that plaque morphology features and critical mechanical condition should be considered in an integrative way for a more accurate vulnerability assessment.

However, the clinical applicability of numerical simulations has been partially impeded by a lack of data regarding the mechanical properties of various atherosclerotic plaque components. Direct material measurements from human atherosclerotic tissues are limited (readers are referred to summaries on the direct measurements with atherosclerotic tissue in Refs. [28,29]). In particular, the material properties of lipid and intraplaque haemorrhage/thrombus (IPH/T) have never been explored. This study presents data on the material behaviour of media, FC, lipid and IPH/T using uniaxial extension testing.

2. Materials and methods

2.1. Tissue preparation and testing

Twenty-one patients with symptomatic carotid atherosclerotic diseases who were scheduled for CEA were recruited consecutively. The patient demographics are listed in Table 1. The study was approved by the local ethics committee, with all patients giving written informed consent. Carotid plaques were collected during surgery and banked in liquid nitrogen for <4 months prior to testing. Cryoprotectant solution (20% dimethylsulfoxide (DMSO) in 5% human albumin solution) added to a final concentration of 10% DMSO was used to prevent ice crystals damaging the tissue. Prior to testing, samples were thawed in a 37 °C tissue bath and cut into rings 1–2 mm thick perpendicular to the blood flow direction from proximal (closer to the heart) to distal, using a scalpel. Approximately 10 rings were obtained from each plaque, and alternate rings were used for material testing. Each ring was further dissected to separate different atherosclerotic tissue components along the ring under a stereo microscope using fine ophthalmic clamps and scissors (Figs. 1–3). The tissue strips were prepared carefully to minimise variation in width and thickness along the length. FC and media were relatively easy to identify and separate; lipid appeared yellow or yellowish, based on visual inspection (Fig. 2); and red or erythroid brown was classified as IPH or thrombus (Fig. 3).

Table 1
Patient demographics (n = 21).

Male, n (%)	18 (85.7)
Age (mean ± SD)	68.2 ± 7.4
Hypertension, n (%)	19 (90.5)
Coronary artery disease, n (%)	6 (28.6)
Diabetes mellitus, n (%)	4 (19.0)
Previous use of statin, n (%)	12 (57.1)
NASCET defined stenosis (%)	72.3 ± 17.0

An in-house-designed tester, consisting of a stepper motor (Miniature Steel Linear Stages, Newport Corporation, USA), load cell (custom designed), camera (PixeLink PL-B776U 3.1 MP USB2 Colour Camera, PixeLINK, Canada) and controlling system developed in LabView 2011 (National Instruments, USA), was used to perform the uniaxial extension tests. The position resolution of the stepper motor was 0.1 μm; the precision of the load cell was 0.0005 N, and the measuring range was 2 N; the image size was 2048 × 1536 pixels, with an 80 × 60 mm^2 field of view. The tissue strip was mounted on the tester using modified 6-cm straight haemostatic clamps (Shanghai Medical Instruments (Group) Ltd., Corp. China). The clamped section of each end was 1–1.5 mm. After five preconditioning cycles (by moving one of the clamps 2.5% of the total distance between the two clamp ends at a speed of 0.05 mm s^{-1}), the testing was performed with a speed of 0.01 mm s^{-1} in a 37 °C saline bath with a 0.005 N pre-loading. Waterproof black ink markers were placed on the surface to trace local displacement. The centre of each marker was identified, and the local stretch ratio was calculated from the distance between the centres. The Cauchy stress was converted from the measured force signal using the strip thickness, the width at rest and the stretch ratio, with the material being assumed to be incompressible.

2.2. Data processing

A modified Mooney–Rivlin strain energy density function was used to characterize the stretch–stress relationship of each tissue type:

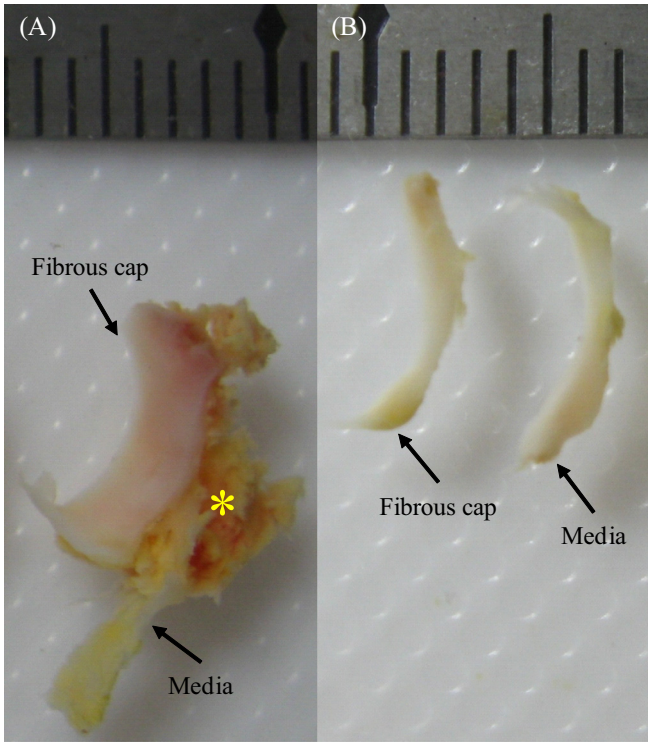

Fig. 1. A representative tissue section with FC and media: (A) the intact section with FC, media and lipid marked by a yellow asterisk; (B) isolated tissue strips of FC and media.

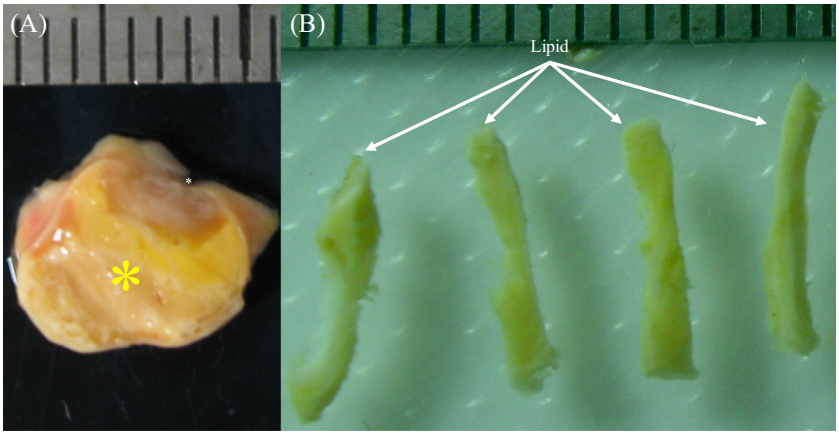

Fig. 2. A representative tissue ring with a big lipid core: (A) the ring from the severe stenotic site; (B) isolated lipid strips; lipid was marked by a yellow asterisk and lumen by a white asterisk.

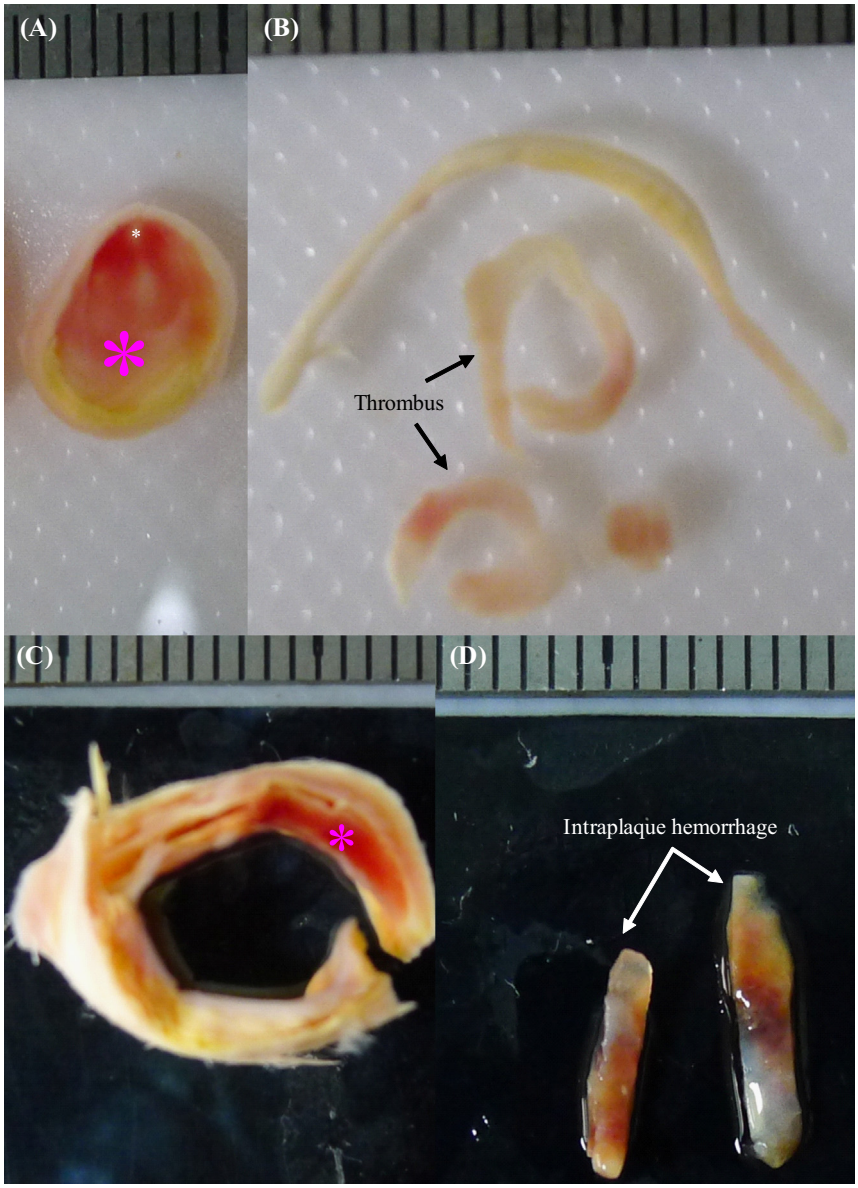

Fig. 3. Nearly occluded plaque ring with recent thrombus and a section with IPH: (A) the ring with a big thrombus; (B) isolated thrombus strips; (C) the section with intraplaque; (D) isolated IPH strip; thrombus and IPH were marked by pink asterisks and lumen was marked by a white asterisk.

$$W = c_1(I_1 - 3) + D_1[e^{D_2(I_1-3)} - 1] + K(J-1)$$

in which I_1 and J are the first invariant and Jacobian of the deformation gradient tensor, respectively; D_1 and D_2 are material constants, and K is the Lagrange multiplier for the incompressibility. Material constants were obtained by minimising the following objective function

$$S = \sum_{i=1}^{N} |\sigma_i - \sigma_i^e|$$

and relative error was used to assess the fitting quality

$$\gamma = \frac{\sum_{i=1}^{N} |\sigma_i - \sigma_i^e|}{\sum_{i=1}^{N} |\sigma_i^e|} \times 100\%$$

in which σ_i and σ_i^e are the predicted and measured stress, respectively; and N is the number of data points. In order to obtain a single constant set of each tissue type for the convenience of computational simulation, in this study, stretch and stress were both averaged in small energy intervals. The elastic energy at each stretch level was defined as

$$W(\lambda) = \int_1^{\lambda} \sigma(\lambda) d\lambda$$

in which σ is the Cauchy stress at the stretch level of λ. For each type of tissue, 100 equal distance intervals were placed between maximum [$\max(W_i(\lambda_i)$] and minimum [$\min(W_i(\lambda_i)$] energy levels, and stretch and stress within each of them were averaged. To avoid bias, intervals with at least five data points from different tissue strips were used for further analysis.

2.3. Statistical analysis

As multiple measurements were obtained from a single plaque, a linear mixed-effect model was used to assess the difference between parameters of different tissue types. All statistical analyses were performed in R 2.10.1 (The R Foundation for Statistical Computing), with statistical significant assumed if $P < 0.05$.

3. Results

In total, 65 media strips from 17 samples, 59 FC strips from 14 samples, 38 lipid strips from 11 samples, and 21 IPH/T strips from 11 samples were collected and tested successfully. For each plaque sample, 8.7 ± 2.1 tissue strips were tested. The thickness, width and length of tissue strips are: media, 0.91 ± 0.30, 1.85 ± 0.41, 15.00 ± 4.21; FC, 0.97 ± 0.26, 1.82 ± 0.47, 12.30 ± 3.22; lipid, 1.28 ± 0.42, 1.74 ± 0.59, 9.92 ± 2.10; and IPH/T, 1.31 ± 0.32, 1.62 ± 0.37, 9.77 ± 3.02 (unit, mm). It is essential to minimise the variation in width and thickness of tissue strip along the length

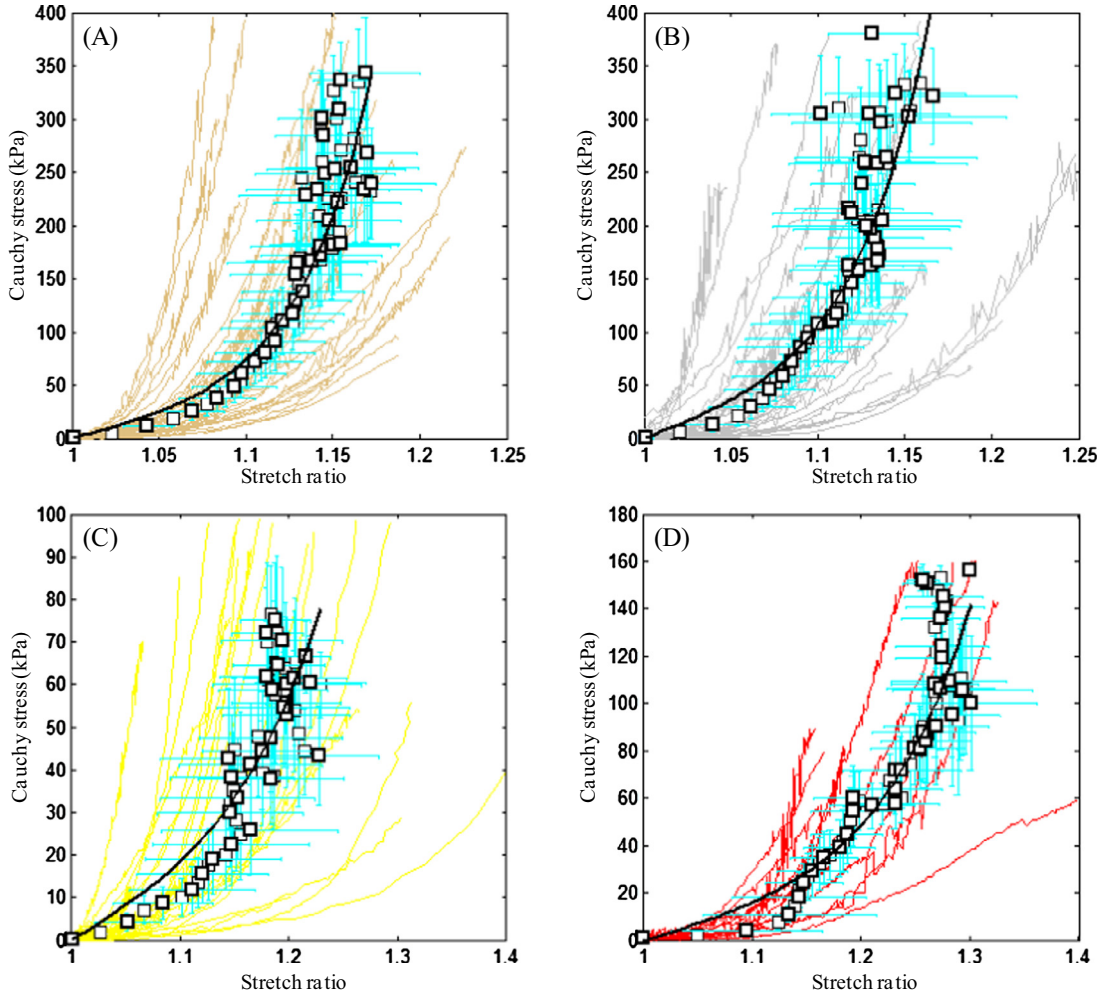

Fig. 4. The stretch–stress curve of each strip from each tissue type and the corresponding averaged data points (black points) with error bars and fitted curves (black lines): (A) media; (B) FC; (C) lipid; (D) IPH/thrombus.

as Cauchy stress was computed by considering these two measurements and the assumption of incompressibility. In this study, the variation (=standard deviation/mean × 100%) in thickness and width of media were 11.8 ± 5.2% and 7.0 ± 3.8%, respectively; those of FC were 12.7 ± 6.3% and 7.0 ± 3.4%, respectively; those of lipid were 8.4 ± 4.0% and 4.9 ± 1.6%, respectively; and those of IPH/T were 9.7 ± 4.2% and 6.7 ± 2.1%, respectively. The test was stopped when the tissue strip slid or broke at the stretch ratio of: media, 1.14 [1.10, 1.19]; FC, 1.13 [1.09, 1.20]; lipid, 1.15 [1.10, 1.26] and IPH/T, 1.30 [1.17, 1.33] (median [inter quartile range]). It can be seen from Fig. 4 that stress–stretch curves usually are not smooth. This generally represents tearing or failure of the tissue when stretched. Each curve and corresponding images taken during the stretching were inspected carefully, and the data points generated after an identifiable tear or sliding were excluded for final analysis.

All tissue types, including lipid and IPH/T, displayed non-linear stretch–stress behaviour, showing an increased stiffness with stretching (Fig. 4). A modified Mooney–Rivlin strain energy density function was able to capture these stretch–stress relationships (Fig. 4). It was found that the material behaviour of each tissue type was not only patient-dependent, but also location-dependent. The averaged data point at each energy interval for each tissue type and the corresponding fitting curve (line in black) are plotted in Fig. 4. The material constants of each tissue type were: media, c_1 = 0.138 kPa, D_1 = 3.833 kPa and D_2 = 18.803 (γ = 19.1%); FC, c_1 = 0.186 kPa, D_1 = 5.769 kPa and D_2 = 18.219 (γ = 19.6%); lipid, c_1 = 0.046 kPa, D_1 = 4.885 kPa and D_2 = 5.426 (γ = 21.1%); and IPH/T, c_1 = 0.212 kPa, D_1 = 4.260 kPa and D_2 = 5.312 (γ = 17.5%). As indicated by D_2, both media and FC are much stiffer than either lipid or IPH/T ($P < 0.05$). This comparison is shown in Fig. 5.

Considering the non-linearity of each tissue type, the incremental elastic modulus

$$E(\lambda) = \frac{d\sigma}{d\lambda}$$

was used for a quantitative comparison. As listed in Table 2, the incremental elastic moduli of media and FC were comparable at different stretch levels, as were lipid and IPH/T ($P > 0.05$). The values of media and FC were all significantly higher than either lipid or IPH/T ($P < 0.05$).

4. Discussion

The present study directly quantified the material properties, in the circumferential direction, of media, FC, lipid and IPH/T from human carotid atherosclerotic plaques. The results highlight that all these tissues exhibit non-linear behaviour, showing increased stiffness while stretched (Figs. 4 and 5 and Table 2). The stiffness of media and FC at all stretch levels in the range 1.0–1.2 were comparable ($P > 0.05$), and the same observation is found between lipid and IPH/T. However, the stiffness of media or FC was significantly higher than that of either lipid or IPH/T.

Owing to the difficulty in obtaining patient-specific material properties for each atherosclerotic plaque component, a single set of material constants is used for all patients in clinically orientated studies. This study proposed to average the stretch and stress within each small elastic energy interval to produce a set of material constants for each tissue type. Other averaging strategies, such as stretch-based and stress-based intervals, have also been tried. For a stretch-based interval, the stretch range was divided into 100 equal-distance intervals, and stress values within each interval were averaged (black data points in Fig. 6; every other point is plotted); and for stress-based intervals, intervals were created within the stress range, and stretches were averaged (blue data points in Fig. 6; every other point is plotted). By comparing data points, the energy-based processing approach (green data points in Fig. 6; every other point is plotted) may be the most suitable to generate the representative curve. There was no significant difference in fitting if 80 or 120 intervals were used.

It should be noted that the fitting results for each curve depend on the initial guessed values, i.e. there are multi sets of c_1, D_1 and D_2, which can all fit the stress–stretch curve well (Fig. 7). Therefore, either median or mean values of the constants for each tissue strip

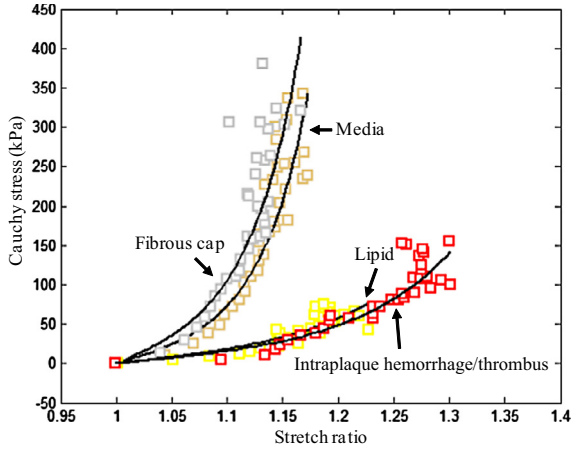

Fig. 5. Comparison of averaged data points and fitted curve from each tissue type. Media and FC show similar material behaviour; both lipid and IPH/thrombus are much softer.

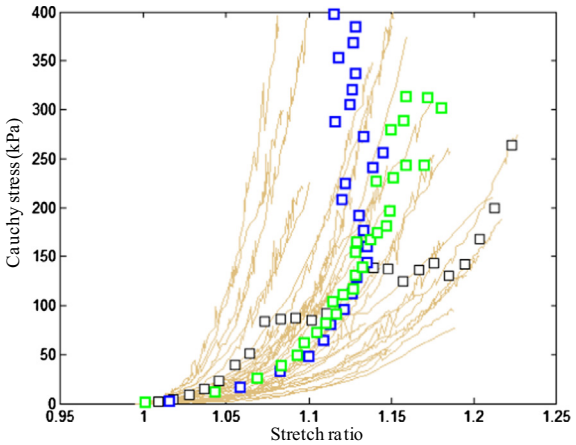

Fig. 6. The averaged data points of media obtained using different averaging strategies: black, averaged within intervals of stretch ratio; blue, averaged within intervals of stress; and green, averaged within intervals of energy.

Table 2
Incremental elastic modulus $E(\lambda)$ for each tissue type at differing stretch levels (unit, kPa; median [inter quartile range]).

Tissue type	λ = 1	λ = 1.05	λ = 1.1	λ = 1.15
Media	290.1 [75.3, 561.5]	379.6 [121.1, 1106.5]	1019.5 [257.1, 2960.2]	4302.7 [1216.8, 8791.7]
Fibrous cap	244.5 [134.7, 517.8]	347.3 [189.6, 804.9]	817.4 [359.0, 2698.0]	3335.0 [825.5, 11721.2]
Lipid	104.4 [31.6, 270.0]	173.4 [47.5, 384.3]	220.7 [78.0, 549.4]	533.4.4 [195.1, 1060.1]
IPH/T	52.9 [27.6, 133.7]	72.3 [38.0, 157.6]	176.9.0 [45.3, 281.7]	268.8 [58.5, 699.8]

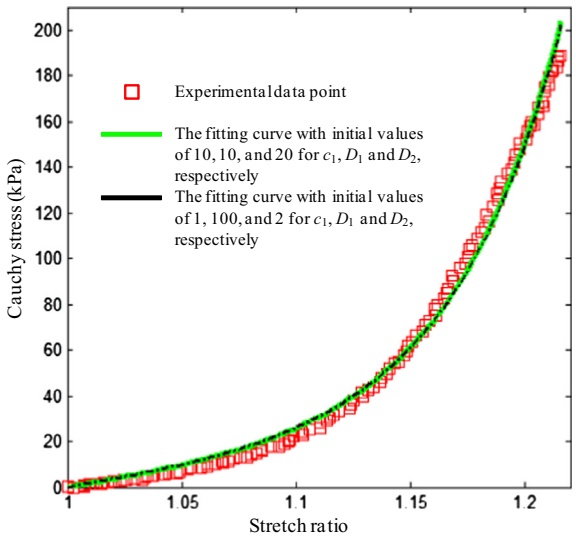

Fig. 7. Different sets of material constants can fit an experimental curve well. The constants for line in green are: $c_1 = 9.495 \times 10^{-8}$, $D_1 = 2.155$ kPa, $D_2 = 13.570$ and $\gamma = 5.6\%$; and those for black line are: $c_1 = 0.650$, $D_1 = 2.167$ kPa, $D_2 = 13.499$ and $\gamma = 5.5\%$.

could not be an adequate representation for each tissue type, as local minimisation is achieved in fitting the experimental curve.

Previously reported studies focused mainly on the material behaviour of FC or whole plaques, while lipid, IPH and thrombus have been assessed less (Table 3). As shown in Table 2, both media and FC are relatively stiff materials. The median values of incremental Young's modulus of media and FC at $\lambda = 1$ are 290.1 kPa and 244.5 kPa, respectively, and they increase to 1019.5 kPa and 817.4 kPa at $\lambda = 1.1$. These values are larger than some previously reported values of Young's modulus (Table 3), but comparable with the values reported by Learoyd and Taylor [30]. Such variability may be attributable to the method of tissue preparation and testing used in the studies. If a whole plaque sample was tested under extension, due to the 'C' shape of the tissue sample, the stretch ratio could be overestimated, as the displacement induced by bending could be misinterpreted as tissue stretching. Moreover, whole plaque samples are usually thick, wide and inhomogeneous, not all parts can be stretched simultaneously, and therefore only a part of the tissue would contribute to the loading. This could underestimate stress when measured force is averaged over the cross section. Either or both of these factors could lead to an underestimation of Young's modulus. Alternatively, if indentation testing is used, only tissue behaviour in compression is assessed, which would not be sufficient for fibre-orientated materials where the fibres' extension characterises the main feature of their mechanical properties. Expansion tests with whole plaques could avoid these limitations partially, but cannot assess the material behaviour of each individual plaque component.

In this study, although some lipid and IPH/T were very fragile and unstable, some were strong and flexible, such as those shown in Figs. 2, 3 and 8, permitting uniaxial testing. During the preparation process, fresh IPH was observed to dissolve easily in the saline solution. Therefore, the IPH/T tested in this study was unlikely to be acute, but more likely recent (more than 1 week old). Different testing strategies should be adopted for these friable tissues, with the most appropriate probably being indentation testing.

Considering the dramatic change in Young's modulus for each atherosclerotic component in a small stretching range, it would be inappropriate to treat any of these as a linear material. This non-linear behaviour is determined by their inherent microstructure. All soft atherosclerotic components, including FC, lipid and IPH/T, are complicated fibre-based materials. The predominant component of media and FC is connective tissue matrix proteins, particularly collagen types I and III, but also elastin and proteoglycan. Lipid is a mixture of cholesterol clefts and collagen, with part of it deriving from erythrocyte membrane cholesterol [31], which is the debris of blood contents. IPH/T appears to be a complex, age-dependent material. IPH is thought to be caused by

Table 3
Studies of direct material measurements on human carotid atherosclerotic plaques.

Author	Samples (n)	Method	Tissue type	Main conclusions
Learoyd and Taylor [30]	7	Expansion	Whole plaque	Incremental Young's modulus at internal pressure of 40 mmHg was about 250 kPa, at 110 mmHg was 1000 kPa and at 160 mmHg was 3000 kPa
Ebenstein et al. [37]	10	Nano-indentation	Hematoma and fibrous tissue	Young's modulus of hematoma was 230 ± 210 kPa and the one of fibrous tissue was 270 ± 150 kPa
Teng et al. [38]	6	Uniaxial extension	Intima thickness with/without small lipid	The material strength of adventitia was 1996 ± 867 kPa and 1802 ± 703 kPa in the axial and circumferential directions respectively and the corresponding value of media was 519 ± 270 kPa and 1230 ± 533 kPa. Adventitia, media and intact specimens exhibited similar extensibility at failure
Maher et al.[39]	14	Indentation and uniaxial extension	Not mentioned	Calcified plaques had the stiffest response, while echolucent plaques were the least stiff
Barrett et al. [40]	8	Indentation	FC	The inferred shear modulus was found to be in the range 7–100 kPa with a median value of 11 kPa
Lawlor et al. [41]	14	Uniaxial extension	Whole plaque	Experimental Green strains at rupture varied from 0.299 to 0.588 and the Cauchy stress observed in the experiments was between 131 and 779 kPa
Kural et al. [42]	5	Biaxial test	Not mentioned	The Young's modulus was 0.91–4.64 kPa in longitudinal direction and 1.32–6.38 kPa in circumferential direction
Chai et al. [43]	8	Indentation	FC and lipid	Young's modulus of fibrous tissue was found in the range from 6 to 891 kPa (median 30 kPa) and the one of lipid ranged from 9 to 143 kPa (median 16 kPa)
Mulvihill et al. [44]	25	Uniaxial extension	Whole plaque	Rupture stress value for the lipid-dominated plaques is 342 ± 160 kPa and the value for stiffer plaques (calcium to lipid ratio >1) is 618 ± 230 kPa
This study	21	Uniaxial extension	FC, media, lipid and intraplaque hemorrhage/thrombus (IPH/T)	The stiffness of FC and media was comparable and so was lipid and IPH/T. Both FC and media were much stiffer than either lipid or IPH/T

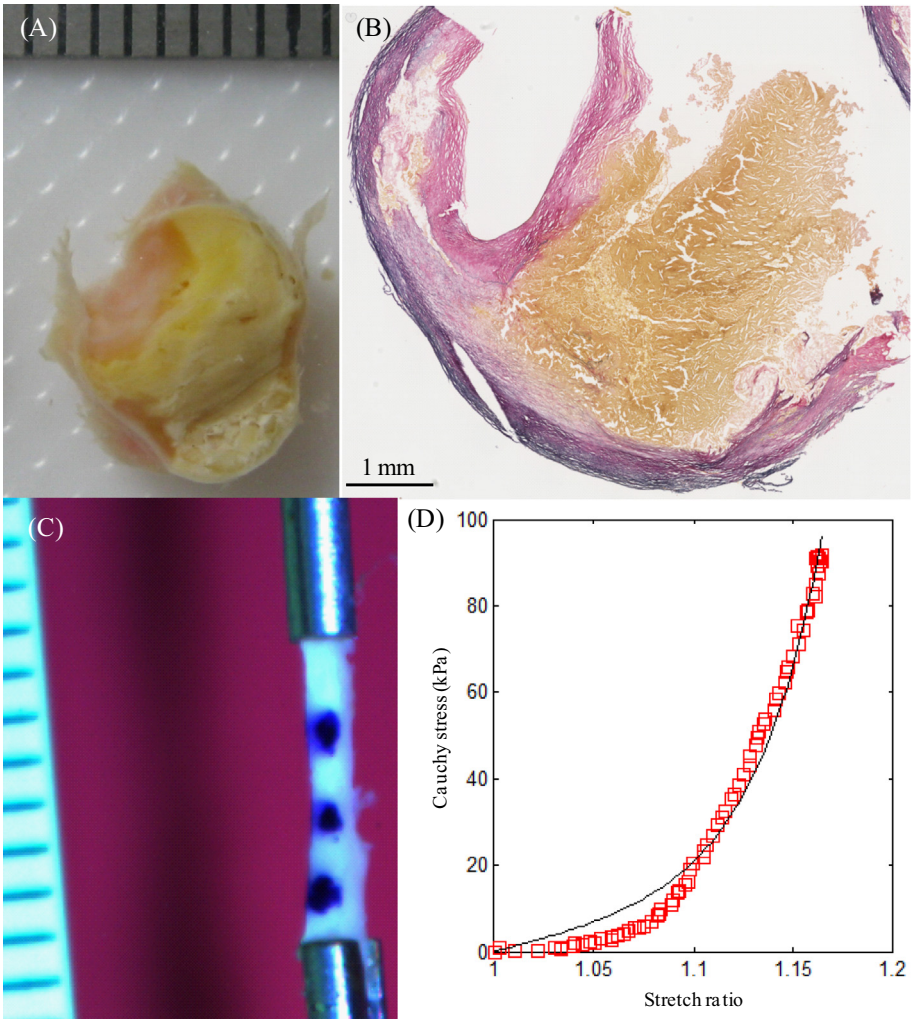

Fig. 8. Certain regions of lipid were not fragile and could undergo testing: (A) the ring with a big lipid core next to the one for material test; (B) the corresponding histological slice confirming the lipid content; (C) one of the lipid strips stretched; (D) the stretch–stress curve of the strip shown in (C); lipid is marked by a yellow asterisk and lumen by a black asterisk.

erythrocyte and plasma leakage from dysfunctional intraplaque neovessels [32]. Once inside the plaque, erythrocytes rapidly undergo lipid peroxidation, followed by phagocytosis via macrophages [33]. The primary trigger of carotid thrombus is FC rupture. Platelet activation and fibrin deposition occur following endothelial disruption and through the exposure of intra-plaque thrombogenic factors [34]. The thrombus may ultimately remain in place, with a new FC forming over the structure [35,36], leading to plaque progression. In the plaque structure, various synthesis, decomposition and secretion processes occur, e.g. inflammatory cells change the structure by secreting cytokines and proteolytic enzymes into the extracellular matrix, resulting in both decreased synthesis and enhanced destruction of extracellular matrix. These pathological processes are patient-, location- and time-dependent, which may explain the large variability of material properties both within and between studies.

As atherosclerotic plaques are heterogeneous structures, it can be challenging to identify and separate each tissue component. Prior to material testing, sample rings were chosen for training, assessing the accuracy of operators to identify and separate plaque component type through visual and histological means. In order to isolate a component, such as FC (Fig. 9A) or media (Fig. 9B), an initial small cut was made at the interface, using fine scissors, and the two parts were separated carefully using fine tweezers (Fig. 9A). Histology examination was then used to confirm tissue type (Fig. 9D and E). Compared with IPH, it was relatively easier to identify thrombus and/or lipid. Thrombus typically appeared as a section of red/reddish substance obstructing the lumen (Fig. 3A), while lipid was yellowish in colour (Fig. 2A and Fig. 8A and B). IPH was a mixture of blood content, lipid and fibrous tissue (Fig. 3D) and was frequently located directly under FC (Fig. 9C and F).

There are inherent limitations in the present study, owing to the unique complexity of atherosclerotic plaques, namely: (1) only material properties in the circumferential direction were assessed; (2) some tissue strips, particularly lipid and IPH/T, may contain more than one tissue type, owing to the highly heterogeneous nature of atherosclerotic plaques. Although the authors attempted to dissect tissue strips by careful inspection using a stereo microscope, potential for tissue misclassification remains; (3) the influence of the tissue microstructure, including fibre orientation, has not been considered; and (4) although cryoprotectant solution had been used in an effort to minimise ice crystal formation, there was still potential for tissue damage during the freezing and storage process. The tissue properties presented here may therefore differ slightly from those obtained from fresh samples.

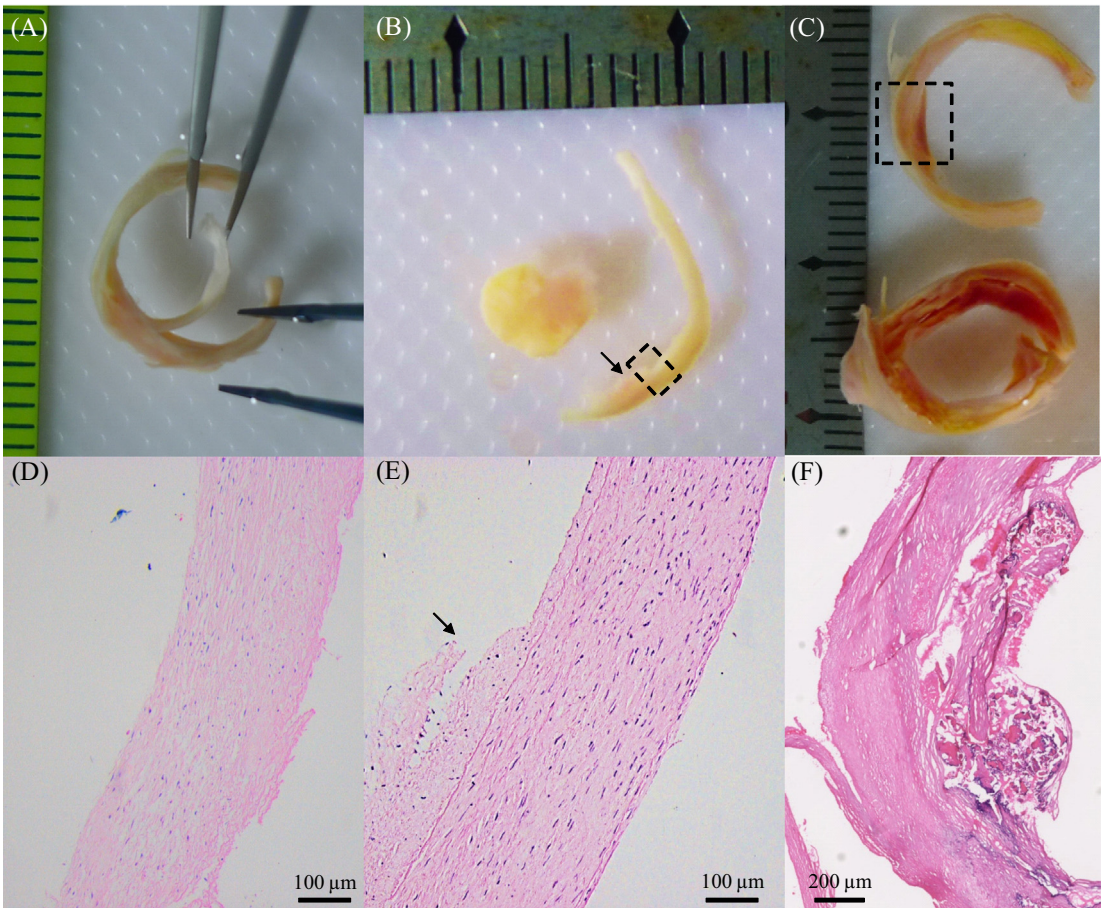

Fig. 9. Separation of FC and media and the identification of FC, media and IPH using histology (H&E stain): (A) partially separated FC; (B) separated media with a small bit of connective fibrous tissue attached (marked by the arrow); (C) two adjacent rings with red/reddish IPH under FC (the one on the bottom is the same one shown in Fig. 3C); (D) the histology examination confirmed that the separated piece shown in (A) was fibrous tissue; (E) the histological result of the region enclosed by the dash-box in (B) showing well-organized media with less organized fibrous tissue attached (arrow); (F) the histology confirmed that the red part enclosed by the dash-in (C) was IPH under a very thin FC.

5. Conclusions

All soft atherosclerotic components in carotid plaques exhibit non-linear behaviour, with both media and FC being stiffer than either lipid or IPH/T. The stiffness of media and FC are comparable, as are the stiffness of lipid and IPH/T. The material constants in the modified Mooney–Rivlin strain energy density function of each tissue type are suggested to be: media, c_1 = 0.138 kPa, D_1 = 3.833 kPa and D_2 = 18.803; FC, c_1 = 0.186 kPa, D_1 = 5.769 kPa and D_2 = 18.219; lipid, c_1 = 0.046 kPa, D_1 = 4.885 kPa and D_2 = 5.426; and IPH/T, c_1 = 0.212 kPa, D_1 = 4.260 kPa and D_2 = 5.312.

Disclosure

The authors do not have any conflict of interest to be declared.

Acknowledgements

This research is supported by BHF PG/11/74/29100 and the NIHR Cambridge Biomedical Research Centre.

Appendix A. Figures with essential colour discrimination

Certain figures in this article, particularly Figs. 1–9, are difficult to interpret in black and white. The full colour images can be found in the on-line version, at http://dx.doi.org/10.1016/j.actbio.2014.09.001.

References

[1] WHO. The Global Burden of Disease: 2004 update. Geneva: WHO; 2008.
[2] Levy EI, Mocco J, Samuelson RM, Ecker RD, Jahromi BS, Hopkins LN. Optimal treatment of carotid artery disease. J Am Coll Cardiol 2008;51:979–85.
[3] Barnett HJ, Taylor DW, Eliasziw M, Fox AJ, Ferguson GG, Haynes RB, et al. Benefit of carotid endarterectomy in patients with symptomatic moderate or severe stenosis. North American Symptomatic Carotid Endarterectomy Trial Collaborators. N Engl J Med 1998;339:1415–25.
[4] Rothwell PM, Gutnikov SA, Warlow CP. Reanalysis of the final results of the European Carotid Surgery Trial. Stroke 2003;34:514–23.
[5] Yuan C, Zhang SX, Polissar NL, Echelard D, Ortiz G, Davis JW, et al. Identification of fibrous cap rupture with magnetic resonance imaging is highly associated with recent transient ischemic attack or stroke. Circulation 2002;105:181–5.
[6] Chu B, Kampschulte A, Ferguson MS, Kerwin WS, Yarnykh VL, O'Brien KD, et al. Hemorrhage in the atherosclerotic carotid plaque: a high-resolution MRI study. Stroke 2004;35:1079–84.
[7] Sadat U, Weerakkody RA, Bowden DJ, Young VE, Graves MJ, Li ZY, et al. Utility of high resolution MR imaging to assess carotid plaque morphology: a comparison of acute symptomatic, recently symptomatic and asymptomatic patients with carotid artery disease. Atherosclerosis 2009;207:434–9.
[8] Eliasziw M, Streifler JY, Fox AJ, Hachinski VC, Ferguson GG, Barnett HJ. Significance of plaque ulceration in symptomatic patients with high-grade carotid stenosis. North American Symptomatic Carotid Endarterectomy Trial. Stroke 1994;25:304–8.
[9] Altaf N, Daniels L, Morgan PS, Auer D, MacSweeney ST, Moody AR, et al. Detection of intraplaque hemorrhage by magnetic resonance imaging in symptomatic patients with mild to moderate carotid stenosis predicts recurrent neurological events. J Vasc Surg 2008;47:337–42.

[10] Takaya N, Yuan C, Chu B, Saam T, Underhill H, Cai J, et al. Association between carotid plaque characteristics and subsequent ischemic cerebrovascular events: a prospective assessment with MRI – initial results. Stroke 2006;37:818–23.
[11] Singh N, Moody AR, Gladstone DJ, Leung G, Ravikumar R, Zhan J, et al. Moderate carotid artery stenosis: MR imaging-depicted intraplaque hemorrhage predicts risk of cerebrovascular ischemic events in asymptomatic men. Radiology 2009;252:502–8.
[12] Gao P, Chen ZQ, Bao YH, Jiao LQ, Ling F. Correlation between carotid intraplaque hemorrhage and clinical symptoms: systematic review of observational studies. Stroke 2007;38:2382–90.
[13] Saam T, Hetterich H, Hoffmann V, Yuan C, Dichgans M, Poppert H, et al. Meta-analysis and systematic review of the predictive value of carotid plaque hemorrhage on cerebrovascular events by magnetic resonance imaging. J Am Coll Cardiol 2013;62:1081–91.
[14] Milei J, Parodi JC, Ferreira M, Barrone A, Grana DR, Matturri L. Atherosclerotic plaque rupture and intraplaque hemorrhage do not correlate with symptoms in carotid artery stenosis. J Vasc Surg 2003;38:1241–7.
[15] Teng Z, Sadat U, Huang Y, Young VE, Graves MJ, Lu J, et al. In vivo MRI-based 3D mechanical stress–strain profiles of carotid plaques with juxtaluminal plaque haemorrhage: an exploratory study for the mechanism of subsequent cerebrovascular events. Eur J Vasc Endovasc Surg 2011;42:427–33.
[16] Teng Z, Sadat U, Brown AJ, Gillard JH. Plaque haemorrhage in carotid artery disease; pathogenesis, clinical and biomechanical considerations. J Biomech 2014;47:847–58.
[17] Sadat U, Teng Z, Young VE, Walsh SR, Li ZY, Graves MJ, et al. Association between biomechanical structural stresses of atherosclerotic carotid plaques and subsequent ischaemic cerebrovascular events – a longitudinal in vivo magnetic resonance imaging-based finite element study. Eur J Vasc Endovasc Surg 2010.
[18] U-King-Im JM, Young V, Gillard JH. Carotid-artery imaging in the diagnosis and management of patients at risk of stroke. Lancet Neurol 2009;8:569–80.
[19] Cheng GC, Loree HM, Kamm RD, Fishbein MC, Lee RT. Distribution of circumferential stress in ruptured and stable atherosclerotic lesions. A structural analysis with histopathological correlation. Circulation 1993;87:1179–87.
[20] Li ZY, Howarth S, Trivedi RA, UK-I JM, Graves MJ, Brown A, et al. Stress analysis of carotid plaque rupture based on in vivo high resolution MRI. J Biomech 2006;39:2611–22.
[21] Sadat U, Li ZY, Graves MJ, Tang TY, Gillard JH. Noninvasive imaging of atheromatous carotid plaques. Nat Clin Pract 2009;6:200–9.
[22] Richardson PD, Davies MJ, Born GV. Influence of plaque configuration and stress distribution on fissuring of coronary atherosclerotic plaques. Lancet 1989;2:941–4.
[23] Sadat U, Li ZY, Young VE, Graves MJ, Boyle JR, Warburton EA, et al. Finite element analysis of vulnerable atherosclerotic plaques: a comparison of mechanical stresses within carotid plaques of acute and recently symptomatic patients with carotid artery disease. J Neurol Neurosurg Psychiatry 2010;81:286–9.
[24] Zhu C, Teng Z, Sadat U, Young VE, Graves MJ, Li ZY, et al. Normalized wall index specific and MRI-based stress analysis of atherosclerotic carotid plaques: a study comparing acutely symptomatic and asymptomatic patients. Circ J 2010;74:2360–4.
[25] Sadat U, Teng Z, Young VE, Graves MJ, Gaunt ME, Gillard JH. High-resolution magnetic resonance imaging-based biomechanical stress analysis of carotid atheroma: a comparison of single transient ischaemic attack, recurrent transient ischaemic attacks, non-disabling stroke and asymptomatic patient groups. Eur J Vasc Endovasc Surg 2011;41:83–90.
[26] Sadat U, Teng Z, Young VE, Walsh SR, Li ZY, Graves MJ, et al. Association between biomechanical structural stresses of atherosclerotic carotid plaques and subsequent ischaemic cerebrovascular events – a longitudinal in vivo magnetic resonance imaging-based finite element study. Eur J Vasc Endovasc Surg 2010;40:485–91.
[27] Teng Z, Brown AJ, Calvert PA, Parker RA, Obaid DR, Huang Y, et al. Coronary plaque structural stress is associated with plaque composition and subtype and higher in acute coronary syndrome: the BEACON I (Biomechanical Evaluation of Atheromatous Coronary Arteries) study. Circ Cardiovasc Imaging 2014;7:461–70.
[28] Sadat U, Teng Z, Gillard JH. Biomechanical structural stresses of atherosclerotic plaques. Expert Rev Cardiovasc Ther 2010;8:1469–81.
[29] Walsh MT, Cunnane EM, Mulvihill JJ, Akyildiz AC, Gijsen FJ, Holzapfel GA. Uniaxial tensile testing approaches for characterisation of atherosclerotic plaques. J Biomech 2014;47:793–804.
[30] Learoyd BM, Taylor MG. Alterations with age in the viscoelastic properties of human arterial walls. Circ Res 1966;18:278–92.
[31] Arbustini E, Morbini P, D'Armini AM, Repetto A, Minzioni G, Piovella F, et al. Plaque composition in plexogenic and thromboembolic pulmonary hypertension: the critical role of thrombotic material in pultaceous core formation. Heart 2002;88:177–82.
[32] Teng Z, He J, Degnan AJ, Chen S, Sadat U, Bahaei NS, et al. Critical mechanical conditions around neovessels in carotid atherosclerotic plaque may promote intraplaque hemorrhage. Atherosclerosis 2012;223:321–6.
[33] Kockx MM, Cromheeke KM, Knaapen MW, Bosmans JM, De Meyer GR, Herman AG, et al. Phagocytosis and macrophage activation associated with hemorrhagic microvessels in human atherosclerosis. Arterioscler Thromb Vasc Biol 2003;23:440–6.
[34] Mackman N. Triggers, targets and treatments for thrombosis. Nature 2008;451:914–8.
[35] Svindland A, Torvik A. Atherosclerotic carotid disease in asymptomatic individuals: an histological study of 53 cases. Acta Neurol Scand 1988;78:506–17.
[36] Qiao Y, Farber A, Semaan E, Hamilton JA. Images in cardiovascular medicine. Healing of an asymptomatic carotid plaque ulceration. Circulation 2008;118:e147–8.
[37] Ebenstein DM, Coughlin D, Chapman J, Li C, Pruitt LA. Nanomechanical properties of calcification, fibrous tissue, and hematoma from atherosclerotic plaques. J Biomed Mater Res 2009;91:1028–37.
[38] Teng Z, Tang D, Zheng J, Woodard PK, Hoffman AH. An experimental study on the ultimate strength of the adventitia and media of human atherosclerotic carotid arteries in circumferential and axial directions. J Biomech 2009;42:2535–9.
[39] Maher E, Creane A, Sultan S, Hynes N, Lally C, Kelly DJ. Tensile and compressive properties of fresh human carotid atherosclerotic plaques. J Biomech 2009;42:2760–7.
[40] Barrett SR, Sutcliffe MP, Howarth S, Li ZY, Gillard JH. Experimental measurement of the mechanical properties of carotid atherothrombotic plaque fibrous cap. J Biomech 2009;42:1650–5.
[41] Lawlor MG, O'Donnell MR, O'Connell BM, Walsh MT. Experimental determination of circumferential properties of fresh carotid artery plaques. J Biomech 2011;44:1709–15.
[42] Kural MH, Cai M, Tang D, Gwyther T, Zheng J, Billiar KL. Planar biaxial characterization of diseased human coronary and carotid arteries for computational modeling. J Biomech 2012;45:790–8.
[43] Chai CK, Akyildiz AC, Speelman L, Gijsen FJ, Oomens CW, van Sambeek MR, et al. Local axial compressive mechanical properties of human carotid atherosclerotic plaques-characterisation by indentation test and inverse finite element analysis. J Biomech 2013;46:1759–66.
[44] Mulvihill JJ, Cunnane EM, McHugh SM, Kavanagh EG, Walsh SR, Walsh MT. Mechanical, biological and structural characterization of in vitro ruptured human carotid plaque tissue. Acta Biomater 2013;9:9027–35.